Metastatic bone tumors: Analysis of factors affecting prognosis and efficacy of CT and ^{18}F-FDG PET-CT in identifying primary lesions

HIROFUMI SHIMADA[1], TAKAO SETOGUCHI[2], MASAHIRO YOKOUCHI[1], HIROMI SASAKI[1], YASUHIRO ISHIDOU[3], ICHIRO KAWAMURA[1], MASAHIKO ABEMATSU[2], SATOSHI NAGANO[1] and SETSURO KOMIYA[1]

[1]Department of Orthopaedic Surgery; [2]The Near-Future Locomotor Organ Medicine Creation Course (Kusunoki Kai); [3]Department of Medical Joint Materials, Graduate School of Medical and Dental Sciences, Kagoshima University, Kagoshima 890-8520, Japan

Received April 28, 2014; Accepted May 28, 2014

DOI: 10.3892/mco.2014.326

Abstract. We analyzed the prognostic factors in patients with metastatic bone tumors and evaluated the efficacy of different modalities in identifying the primary lesions. A total of 145 patients with bone metastases who attended the orthopaedic outpatient clinic were included in this study. The most frequent site of bone metastases was the spine. The primary tumor type was differently distributed between patients with a known primary tumor at the first visit and those with an unknown primary lesion. The number of breast cancer cases was statistically significantly lower in the primary-unknown group. However, the number of myeloma cases was significantly higher in the primary-unknown group. Survival was significantly lower in the skeletal-related events (SREs) compared to that in the non-SREs group. Furthermore, survival was significantly worse in patients with a performance status (PS) of ≥2 compared to those with a PS of ≤1 and neurological complications occurred statistically more often in the group with worse PS (≥2). Survival rates were significantly lower in the non-spinal compared to those in the spinal metastatic group. Since the majority of breast cancer patients presented with metastasis in the spine, a breast cancer origin was a positive prognostic factor in patients with spinal metastases. Although there were no significant differences between computed tomography (CT) and ^{18}F-fluoro-2-deoxyglucose (^{18}F-FDG) positron emission tomography (PET)-CT in detecting primary lesions, CT may be the first choice due to its feasibility. In conclusion, lung cancer, SREs and worse PS were adverse prognostic factors for patients with bone metastasis. In addition, CT scans may be more useful for determining the primary lesion of a bone metastasis compared to ^{18}F-FDG PET-CT in a timelier manner.

Correspondence to: Dr Satoshi Nagano, Department of Orthopaedic Surgery, Graduate School of Medical and Dental Sciences, Kagoshima University, 8-35-1 Sakuragaoka, Kagoshima 890-8520, Japan
E-mail: naga@m2.kufm.kagoshima-u.ac.jp

Key words: metastatic bone tumor, skeletal-related events, performance status, prognostic factor, ^{18}F-fluoro-2-deoxyglucose positron emission tomography-computed tomography

Introduction

The recent advances in cancer treatment have improved patient survival. Cancers that have metastasized to the bones are considered to be at an advanced stage. Metastatic bone tumors often promote skeletal-related events (SREs), which include pathological fractures, neurological complications caused by compression of the spinal cord or cauda equina, or hypercalcemia, as well as the need for radiotherapy or surgery of the bone metastasis (1,2). Although the prognosis of patients with certain types of cancer has improved with the recent advances in chemotherapy and radiotherapy, patients with metastatic bone tumors require treatment of the primary lesion as well as anti-SRE assessment, in order to improve their quality of life and prognosis.

Metastatic bone tumors are treated by multidisciplinary teams, in which orthopaedic surgeons play an important role in the diagnosis and treatment of the bone metastasis, as well as in the detection of the primary cancer lesion. A delay in the diagnosis increases the risk of SREs and negatively affects the prognosis. In this regard, we investigated the background of patients with bone metastasis and the factors associated with prognosis. We investigated 145 cases of metastatic bone tumors with respect to the primary lesion, affected bone site and frequency of SREs and evaluated the effectiveness of a single computed tomography (CT) scan of the chest/abdomen/pelvis against that of ^{18}F-fluoro-2-deoxyglucose (^{18}F-FDG) positron emission tomography (PET)-CT scan in detecting the primary lesion of a metastatic bone tumor.

Materials and methods

Patients. In this retrospective study, we reviewed the medical records and imaging results of 145 patients with metastatic bone

tumors who were referred to the Department of Orthopaedic Surgery, Kagoshima University, between 2006 and 2011. The patients included 81 men and 64 women, with a mean age of 65 years (range, 29-87 years) and a mean follow-up of 9 months. A bone scan was performed on 97 patients.

The study protocol was approved by the Ethics Committee on Clinical Research at the Kagoshima University Hospital and all the patients provided written informed consent prior to inclusion.

Evaluation of imaging modalities and patient survival. Two well-trained radiologists reviewed all the bone scan results and compared them with radiographs, CT or magnetic resonance imaging (MRI) scans. The results of the imaging modalities were assessed taking into account clinical symptoms and any positive findings that indicated bone metastasis. To identify the primary lesion, a single chest/abdominal/pelvic CT, ^{18}F-FDG PET-CT and Tl scan were performed on each patient. Following an initial detection of the primary lesion, roentgenogram, MRI, biopsy and formal clinical follow-up were performed to obtain a definitive diagnosis. We examined the frequency of each primary tumor, bone metastatic site and incidence of SREs; we also estimated the survival rate and the detection rate of the original lesion using clinical examinations and evaluated the factors affecting survival. The survival rate was analyzed according to the Kaplan-Meier method. The clinical examinations that were performed to locate the original tumor were also evaluated.

Statistical analysis. Statistical analysis was performed using the Student's t-test or the Chi-square test and analyzed using Microsoft Office Excel software (Microsoft, Redmond, WA, USA). Kaplan-Meier analysis was performed using Kaplan 97 software. $P<0.05$ was considered to indicate statistically significant differences.

Results

Primary lesion and bone metastatic site. We examined the origin of all metastatic bone tumors (145 cases). The most frequent origin of bone metastasis was lung cancer (34 cases, 23%), followed by breast cancer (19 cases, 13%), kidney cancer (10 cases, 7%), liver cancer (10 cases, 7%), thyroid cancer (9 cases, 6%), prostate cancer (9 cases, 6%), colorectal cancer (8 cases, 6%), malignant lymphoma (7 cases, 5%), multiple myeloma (6 cases, 4%), gastric cancer (6 cases, 4%), and bladder cancer (4 cases, 3%) , as previously reported (3-5). The primary tumor could not be identified in 5 cases (3%; Fig. 1A). The Kaplan-Meier analysis demonstrated that the 1-, 2- and 3-year survival rate was 49, 34 and 18%, respectively, among all patients with bone metastasis (Fig. 2).

The most frequent bone metastatic site was the spine (143 cases), including the cervical vertebrae (28 sites), thoracic vertebrae (45 sites), lumbar vertebrae (53 sites) and sacrum (17 sites). Other sites of metastasis included the femur (28 cases), pelvis (27 cases), humerus (16 cases) and ribs (15 cases) (Fig. 1B). Our findings revealed that the most frequent spinal metastatic site was the lumbar spine, followed by the thoracic and cervical spine. It was previously reported that the most frequent metastatic site was the thoracic spine, followed by the lumbar and cervical spine (6-9). To explain this discrepancy, we compared the primary malignant tumor between the lumbar and thoracic metastatic groups. We identified no statistically significant difference in the primary lesion between these two groups.

The primary tumor site distribution was compared between patients with a known primary lesion and those with unknown primary lesion at the first visit. In the primary-known group (n=84), the primary tumors were breast (18 cases, 21%), lung (11 cases, 13%), liver (9 cases, 11%), thyroid (7 cases, 8%) and kidney cancer (6 cases, 7%). In the primary-unknown group (n=61), the primary tumors were lung cancer (23 cases, 38%), myeloma (5 cases, 8%), kidney and prostate cancer and malignant lymphoma (4 cases each, 7%) (Table I). During the follow-up period, the primary lesion was not identified in 5 cases. The number of breast cancer cases was statistically significantly lower in the primary-unknown group. However, the number of myeloma was significantly higher in the primary-unknown group.

Factors affecting the prognosis of bone metastasis. We first investigated the association between prognosis and SREs and observed that survival was significantly lower in the SREs compared to that in the non-SREs group (Fig. 3A). In addition, PS was found to be an important factor for the selection of the appropriate chemotherapeutic regimen and, therefore, we investigated the association between patient prognosis and PS (10,11) and survival was found to be significantly lower in the PS≥2 compared to that in the PS≤1 group (Fig. 3B). Since the most frequent bone metastatic site was the spine, we investigated the association between spinal metastasis and patient prognosis. The Kaplan-Meier analysis revealed that the 1- and 3-year survival rates for patients with spinal metastases was 56 and 23%, respectively. Furthermore, the 1- and 3-year survival rates for patients with non-spinal metastases were 37 and 8%, respectively. Therefore, survival rates were significantly lower in the non-spinal compared to those in the spinal metastatic group (Fig. 3C). To determine which factors were associated with a favorable prognosis in patients with spinal metastasis, we investigated the association between prognosis and neurological complications caused by compression of the spinal cord or cauda equina. The Kaplan-Meier analysis revealed that neurological complications did not exert a significant effect on survival for any of the patients with bone metastasis (Fig. 3D). We next investigated the primary lesion in the non-spinal and spinal metastatic groups and found that the number of breast cancer patients was higher in the spinal metastatic group (Table II).

Association between SREs and prognosis or PS. We demonstrated that the survival rate was significantly lower in the PS≥2 compared to that in the PS≤1 group (Fig. 3B). We investigated the association between SREs and PS. The incidence of SREs among all the bone metastatic cases was 107 (74%). Hypercalcemia (serum calcium levels, 10.4-12.6 mg/dl; normal range, 8.5-10.3 mg/dl) occurred in 8 cases (5.5%) and was accompanied by renal dysfunction in 4 of the 8 cases (Table IIIA). Symptoms caused by compression of the spinal cord or cauda equina were observed in 36 cases (24.8%), including symptoms of the cervical (11 cases), thoracic (15 cases) and lumbar segments (10 cases) (Table IIIA and B).

Table I. Comparison of the primary tumor site between groups with known and unknown origin at initial visit.

Origin known at initial visit	Cases (%)	Origin unknown → diagnosed	Cases (%)
Breast	18[a] (21)	Lung	23 (38)
Lung	11 (13)	Myeloma	5[b] (8)
Liver	9 (11)	Kidney	4 (7)
Thyroid	7 (8)	Prostate	4 (7)
Kidney	6 (7)	Lymphoma	4 (7)
Prostate	5 (6)	Gastric	3 (5)
Colorectal	5 (6)	Colorectal	3 (5)
Lymphoma	3 (4)	Thyroid	2 (3)
Esophagus	3 (4)	Pancreas	2 (3)
Gastric	3 (4)	Bladder	2 (3)
Uterus	3 (4)	Breast	1[a] (2)
Tongue	2 (2)	Others	8 (12)
Bladder	2 (2)		
Myeloma	1[b] (1)		
Others	6 (7)		
Total	84 (100)	Total	61 (100)

[a]P<0.01, [b]P<0.05.

Table II. Comparison of the primary tumor site between groups with and without spinal metastasis.

Spinal metastasis (+)	Cases	Spinal metastasis (-)	Cases
Lung	22	Lung	12
Breast	17[a]	Kidney	5
Liver	8	Thyroid	4
Prostate	7	Liver	4
Colorectal	6	Bladder	4
Thyroid	5	Lymphoma	3
Kidney	5	Esophagus	2
Myeloma	5	Gastric	2
Gastric	4	Breast	2[a]
Lymphoma	4	Prostate	2
Pancreas	3	Colorectal	2
Tongue	2	Others	4
Others	11		
Total	99	Total	46

[a]P<0.05.

Pathological fractures were detected in 23 cases (15.9%), including fractures of the extremities (femur, 9 cases; and humerus, 5 cases); thoracic vertebrae, 3 cases; and lumbar vertebrae, 2 cases (Table IIIC). Surgery for SREs was performed in 26 cases (18%), including internal fixation (10 cases), resection plus reconstruction (9 cases), spinal decompression (2 cases), spinal fusion (4 cases) and total en bloc spondylectomy (1 case)

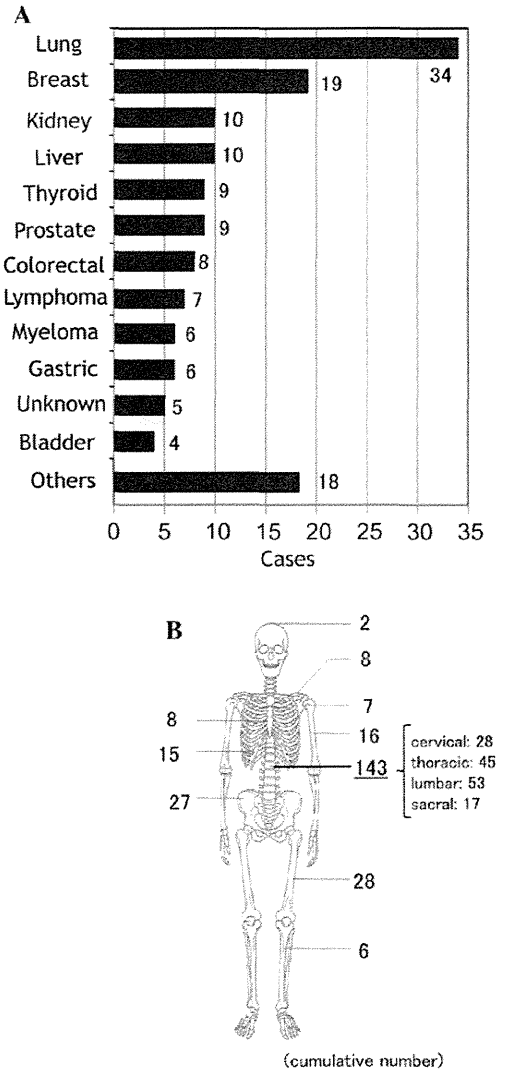

Figure 1. Number of bone metastases. (A) Number of cases with bone metastases per primary lesion. (B) Number of patients per bone metastatic site.

(Table IIID). Radiotherapy for bone metastasis was performed in 75 cases (51.7%).

In the group with better PS scores (≤1, n=32), pathological fractures were detected in 3 cases (9.4%), neurological complications were observed in 3 cases (9.4%), hypercalcemia occurred in 2 cases (6.3%), surgery for SREs was performed in 4 cases (12.5%) and radiotherapy was performed in 14 cases (43.8%). In the group with poor PS scores (≥2, n=113), pathological fractures were detected in 20 cases (17.7%), neurological complications caused by compression of the spinal cord or cauda equina were observed in 33 cases (29.2%), hypercalcemia occurred in 6 cases (5.3%), surgery for SREs was performed in 24 cases (21.2%) and radiotherapy was performed in 70 cases (61.9%). Among the 5 SREs, only neurological complications were found to be significantly increased in the group with a PS score of ≥2 compared to that with a PS score of ≤1 (Table IIIE).

Identification of the primary lesion using imaging studies. The primary tumor site was identified using diagnostic imaging in

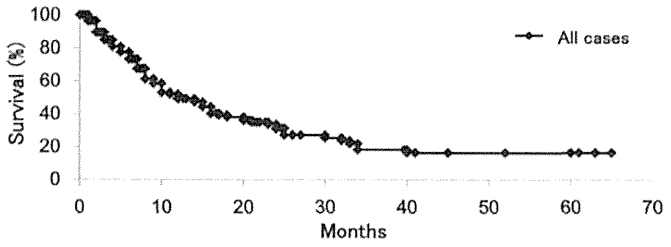

Figure 2. Overall survival rate. The Kaplan-Meier analysis revealed that the 1-, 2- and 3-year survival rates were 49, 34 and 18%, respectively, among all patients with bone metastasis.

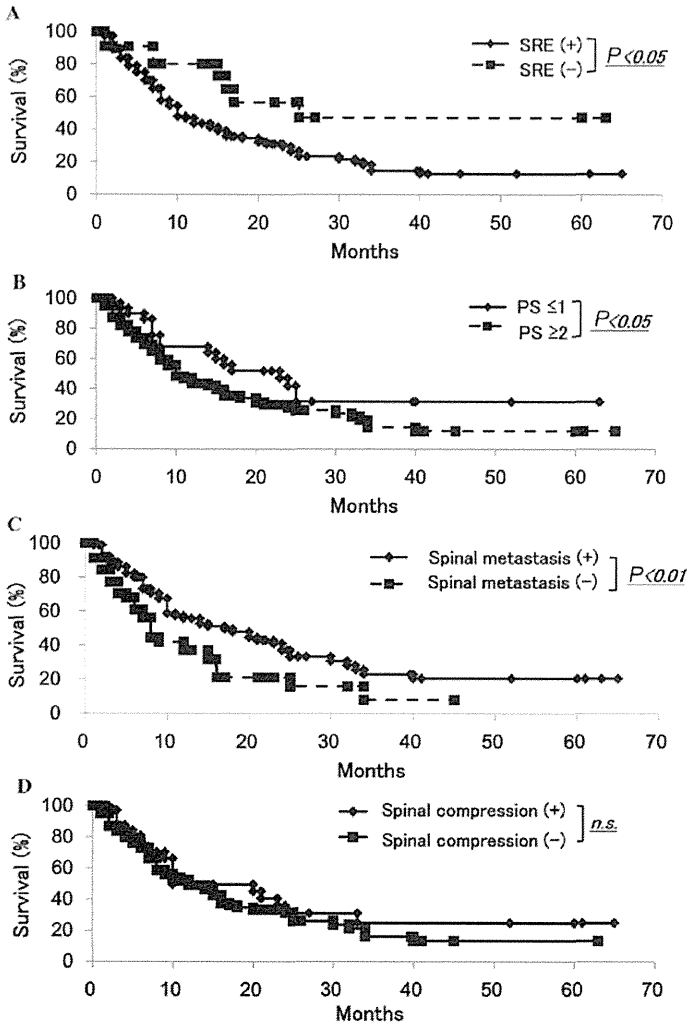

Figure 3. Comparison of survival rates. The Kaplan-Meier analysis revealed that (A) survival was significantly lower in the skeletal-related events (SREs) compared to that in the non-SREs group; (B) survival was significantly lower in the performance status (PS)≥2 compared to that in the PS≤1 group; (C) survival rates were significantly lower in the non-spinal compared to those in the spinal metastatic group; and (D) neurological complications did not exert a significant effect on survival for any bone metastatic patients; n.s., not signifigant.

49 cases, which included CT (32 cases) and ^{18}F-FDG PET-CT (17 cases) (Table IVA). Whole-body bone scans and Tl scans could not identify the primary lesion. CT was performed on 55 patients (90%) in whom the primary tumor was not identified during the first visit to the hospital. The time interval from the first visit until the CT scan was performed was 3.6 days. ^{18}F-FDG PET-CT was performed on 39 patients (64%) with unidentified primary tumors. The time interval from the first visit until the ^{18}F-FDG PET-CT was performed was 7.2 days. CT scans helped identify the following primary cancers: lung (16 cases), kidney (3 cases), thyroid (2 cases), pancreatic (2 cases) and bladder cancer (2 cases), myeloma (2 cases) and others (5 cases). ^{18}F-FDG PET-CT scans identified the following primary cancers: lung (6 cases), prostate (4 cases),

Table III. Analysis of SREs.

A, Number of cases per SRE

Cases	Fracture	Hyper-calcemia	Spinal compression	Radiation therapy for bone metastasis	Surgery for bone metastasis	Total cases with SREs
No. (%)	23 (15.9)	8 (5.5)	36 (24.8)	75 (51.7)	26 (17.9)	107 (73.8)

B, Distribution of spinal metastases in patients with symptoms caused by compression of spinal cord or cauda equina

Cases	Cervical spine	Thoracic spine	Lumbar spine	Total
No. (%)	11 (30.5)	15 (41.7)	10 (27.8)	36 (100)

C, Pathological fractures

Cases	Femur	Humerus	Thoracic spine	Lumbar spine	Others	Total
No. (%)	9 (39.1)	5 (21.7)	3 (13.0)	2 (8.7)	4 (17.5)	23 (100)

D, Type of surgery for pathological fractures

Cases	Resection plus reconstruction	Internal fixation	Spinal fusion	Spinal decompression	Total en bloc spondylectomy	Total
No. (%)	9 (34.6)	10 (38.5)	4 (15.4)	2 (7.7)	1 (3.8)	26 (100)

E, Incidence of SREs in groups with better (≤1) and worse (≥2) PS

Cases, no. (%)	Fracture	Hypercalcemia	Spinal compression	Radiation therapy for bone metastasis	Surgery for bone metastasis
PS≤1 (n=32)	3 (9.4)	2 (6.3)	3 (9.4)[a]	14 (43.8)	4 (12.5)
PS≥2 (n=113)	20 (17.7)	6 (5.3)	33 (29.2)[a]	70 (61.9)	24 (21.2)

SRE, skeletal-related event; PS, performance status. [a]P<0.05.

colorectum (2 cases) and others (5 cases) (Table IVB). A CT scan alone was able to identify primary tumors of the bladder (2 cases), myeloma (2 cases) and thyroid cancer (1 case) that could not be identified using ^{18}F-FDG PET-CT imaging. However, a ^{18}F-FDG PET-CT scan alone was able to identify primary lung cancer (1 case), myeloma (1 case) and colorectal cancer (1 case) (Table IVB). Although there were no significant differences between CT and ^{18}F-FDG PET-CT scans in the detection of primary lesions, CT scans were found to be more useful in determining the primary lesion of a bone metastasis in a timelier manner.

Discussion

Over the last few years, the number of cancer patients has increased. The majority of patients who are diagnosed with bone metastasis are referred to an orthopaedic surgeon to evaluate the bone metastasis and its progression, locate the primary lesion and decide upon treatment options.

We demonstrated that metastasis to the spine was the most frequent, followed by the femur and pelvic bone, as previously reported (6). Of the total bone metastases, the ratio of spinal metastasis was 54.7% (141/258 lesions). Our findings revealed that the number of bone metastases to the spine was lower compared to what was previously reported; in addition, the incidence of lumbar metastasis was relatively high compared to previous reports (6-9,12). Overall survival depends mainly on the type of the primary tumor. We did not identify a statistically significant difference regarding the type of primary tumor between the lumbar and thoracic metastatic groups. The relatively low number of spinal metastases may be the cause of this discrepancy. However, further studies are required to elucidate this issue.

It has been reported that the median overall survival of patients with spinal metastases is 7 months. In addition, only 10-20% of patients with spinal metastases remained alive at 2 years after diagnosis (12). We found that the 1-year survival rate was 49% and the 3-year survival rate was 18% among

Table IV. Comparison of imaging modalities for the identification of the primary lesion in patients with bone metastasis.

A, Time interval for detection of the primary lesion with different imaging modalities

Imaging modality	Detection of primary lesion/total number of patients	Interval between first visit and examination (days)
CT scan	32/55	3.6
PET-CT	17/39	7.2
Bone scan	0/43	6.3
Tl scan	0/13	5.5

B, Number of cases with different primary lesions detected with CT or PET-CT

	Method of identification of primary lesion			
Primary lesion	CT	PET	CT alone	PET alone
Lung	16	6	0	1
Kidney	3	1	0	0
Thyroid	2	0	1	0
Bladder	2	0	2	0
Pancreas	2	0	0	0
Myeloma	2	1	2	1
Gastric	1	1	0	0
Liver	1	1	0	0
Colorectal	1	2	0	1
Lymphoma	1	0	0	0
GIST	1	0	0	0
Prostate	0	4	0	0
Breast	0	1	0	0
Total	32	17	5	3

PET-CT, positron emission tomography-computed tomography.

all patients with bone metastasis. Our results indicated a relatively good prognosis compared to those of a previous study (12). In addition, the survival rates were significantly lower in patients in the non-spinal compared with those in the spinal metastatic group, which included all the patients with bone metastasis. Furthermore, our findings revealed that the number of breast cancer patients was higher in the spinal compared to that in the non-spinal metastatic group. Survival was significantly increased in breast cancer patients with bone metastasis compared to those with other primary lesions with bone metastasis (data not shown). These findings suggest that differences in the origin of the cancer may affect prognosis, depending on whether bone metastasis occurs in the spine or elsewhere.

We demonstrated that SREs exert a significant negative effect on survival. Although neurological complications did not appear to exert a statistically significant effect on survival in patients with spinal metastasis, the number of patients with neurological complications was statistically different between the PS≤1 and PS≥2 groups. These findings suggest that the incidence of neurological complications was increased in the group with PS≥2 and negatively affected survival. In addition, Katagiri *et al* (11) reported that PS scores of 3 or 4 were a significant poor prognostic factor. Our findings suggest that a PS score of 2 may also exert a negative effect on prognosis in patients with bone metastasis.

We observed that the primary lesion distribution differed depending on whether the primary tumor was known or unknown at the initial visit. In the primary-known group, the most frequent primary cancer was breast cancer, followed by lung, liver and thyroid cancer. Our findings suggest the significance of the follow-up of cancer patients with bone metastasis. In the primary-unknown group, the most frequent primary cancer was lung cancer, followed by myeloma, kidney and prostate cancer. Consistent with our results, Iizuka *et al* (4) reported that myeloma was the most common primary malignancy in cases with spinal metastasis of unknown origin, followed by lung and prostate cancer. Destombe *et al* (3) reported that the most frequent primary cancer was lung, followed by breast cancer. These findings suggest that, when evaluating bone metastatic patients with unknown primary tumors, clinical examinations should be performed taking into consideration the possibility of diagnosing these primary cancers. During the follow-up period, the primary lesion was not identified in 5 cases. It was reported that lung and pancreatic cancer were the most frequent primary lesions in autopsy studies (13,14). Our findings demonstrated that pancreatic cancer was diagnosed as the primary lesion in only 2 cases (3%) in the primary-unknown group. These findings suggest that more detailed examinations, including magnetic resonance cholangiopancreatography or endoscopic retrograde cholangiopancreatography, may be required for bone metastatic patients in whom the primary lesion was not identified.

Although biopsy of the most accessible osseous lesion was routine during the examination, the proportion of an accurate final diagnosis in solid and hematopoietic tumors was low (4,5,15). In addition, biopsy requires invasive procedures. ^{18}F-FDG PET-CT whole-body imaging is non-invasive and highly sensitive. It has been reported that ^{18}F-FDG PET-CT should be used as a first-line imaging examination for patients with a primary carcinoma of unknown origin, rather than after other diagnostic procedures have failed to identify the primary lesion (16). Although ^{18}F-FDG PET-CT is useful in helping physicians locate the primary lesion, patients were required to wait an average of 7.2 days for an ^{18}F-FDG PET-CT examination, due to the long waiting list. We demonstrated that CT scans helped identify 32 of the 55 (58%) primary lesions within 3.6 days from the time of the patient's first visit. Therefore, a CT scan is a rapid examination, valuable for the identification of the primary lesion of a bone metastasis. In addition, we did not observe a statistically significant difference in utility between CT and ^{18}F-FDG PET-CT in establishing the origin of a bone metastasis. Our findings suggest that a CT scan should be performed prior to an ^{18}F-FDG PET-CT scan, particularly if the latter requires a waiting period of several days.

To improve the prognosis of patients with metastatic bone tumors, a team approach is required, comprising an orthopaedic surgeon along with a specialist to manage

treatment of the primary tumor, a radiologist, rehabilitation staff and a palliative care team (17). Collaboration is essential to developing a treatment strategy that may be tailored to the individual patient (18). In this regard, our department has established a bone metastasis registration system that encompasses all specialties in our hospital and is accessible to each specialty.

In conclusion, our findings demonstrated that several factors may be related to patient prognosis and the effectiveness of CT; these factors may prove useful in determining the origin of the primary lesion. Further examination of prognostic factors and advancements in diagnostic imaging may improve the treatment of patients with bone metastasis.

References

1. Coleman RE: Bisphosphonates: clinical experience. Oncologist 9 (Suppl 4): 14-27, 2004.
2. Lipton A, Colombo-Berra A, Bukowski RM, Rosen L, Zheng M and Urbanowitz G: Skeletal complications in patients with bone metastases from renal cell carcinoma and therapeutic benefits of zoledronic acid. Clin Cancer Res 10: 6397S-6403S, 2004.
3. Destombe C, Botton E, Le Gal G, *et al*: Investigations for bone metastasis from an unknown primary. Joint Bone Spine 74: 85-89, 2007.
4. Iizuka Y, Iizuka H, Tsutsumi S, *et al*: Diagnosis of a previously unidentified primary site in patients with spinal metastasis: diagnostic usefulness of laboratory analysis, CT scanning and CT-guided biopsy. Eur Spine J 18: 1431-1435, 2009.
5. Katagiri H, Takahashi M, Inagaki J, Sugiura H, Ito S and Iwata H: Determining the site of the primary cancer in patients with skeletal metastasis of unknown origin: a retrospective study. Cancer 86: 533-537, 1999.
6. Kakhki VR, Anvari K, Sadeghi R, Mahmoudian AS and Torabian-Kakhki M: Pattern and distribution of bone metastases in common malignant tumors. Nucl Med Rev Cent East Eur 16: 66-69, 2013.
7. Bartels RH, van der Linden YM and van der Graaf WT: Spinal extradural metastasis: review of current treatment options. CA Cancer J Clin 58: 245-259, 2008.
8. Harel R and Angelov L: Spine metastases: current treatments and future directions. Eur J Cancer 46: 2696-2707, 2010.
9. Sutcliffe P, Connock M, Shyangdan D, Court R, Kandala NB and Clarke A: A systematic review of evidence on malignant spinal metastases: natural history and technologies for identifying patients at high risk of vertebral fracture and spinal cord compression. Health Technol Assess 17: 1-274, 2013.
10. Oken MM, Creech RH, Tormey DC, *et al*: Toxicity and response criteria of the Eastern Cooperative Oncology Group. Am J Clin Oncol 5: 649-655, 1982.
11. Katagiri H, Takahashi M, Wakai K, Sugiura H, Kataoka T and Nakanishi K: Prognostic factors and a scoring system for patients with skeletal metastasis. J Bone Joint Surg Br 87: 698-703, 2005.
12. Delank KS, Wendtner C, Eich HT and Eysel P: The treatment of spinal metastases. Dtsch Arztebl Int 108: 71-80, 2011.
13. Al-Brahim N, Ross C, Carter B and Chorneyko K: The value of postmortem examination in cases of metastasis of unknown origin - 20-year retrospective data from a tertiary care center. Ann Diagn Pathol 9: 77-80, 2005.
14. Blaszyk H, Hartmann A and Bjornsson J: Cancer of unknown primary: clinicopathologic correlations. APMIS 111: 1089-1094, 2003.
15. Rougraff BT, Kneisl JS and Simon MA: Skeletal metastases of unknown origin. A prospective study of a diagnostic strategy. J Bone Joint Surg Am 75: 1276-1281, 1993.
16. Han A, Xue J, Hu M, Zheng J and Wang X: Clinical value of ^{18}F-FDG PET-CT in detecting primary tumor for patients with carcinoma of unknown primary. Cancer Epidemiol 36: 470-475, 2012.
17. Ecker RD, Endo T, Wetjen NM and Krauss WE: Diagnosis and treatment of vertebral column metastases. Mayo Clin Proc 80: 1177-1186, 2005.
18. Sciubba DM, Petteys RJ, Dekutoski MB, *et al*: Diagnosis and management of metastatic spine disease. A review. J Neurosurg Spine 13: 94-108, 2010.

THE JOURNAL OF BIOLOGICAL CHEMISTRY VOL. 289, NO. 14, pp. 9865–9879, April 4, 2014

Human Immunodeficiency Virus Type 1 Enhancer-binding Protein 3 Is Essential for the Expression of Asparagine-linked Glycosylation 2 in the Regulation of Osteoblast and Chondrocyte Differentiation*[S]

Received for publication, September 20, 2013, and in revised form, January 26, 2014 Published, JBC Papers in Press, February 21, 2014, DOI 10.1074/jbc.M113.520585

Katsuyuki Imamura[‡§], Shingo Maeda[‡1], Ichiro Kawamura[§], Kanehiro Matsuyama[‡§], Naohiro Shinohara[‡§], Yuhei Yahiro[‡§], Satoshi Nagano[§], Takao Setoguchi[¶], Masahiro Yokouchi[§], Yasuhiro Ishidou[‡], and Setsuro Komiya[‡§¶]

From the Departments of [‡]Medical Joint Materials and [§]Orthopaedic Surgery and the [¶]Near-Future Locomotor Organ Medicine Creation Course, Graduate School of Medical and Dental Sciences, Kagoshima University, Kagoshima 890-8544, Japan

Background: The mechanisms by which Hivep3 regulates the osteochondrogenesis remain elusive.
Results: Knockdown of Hivep3 down-regulated *Alg2* expression. Alg2 suppressed osteoblast differentiation by inhibiting the activity of Runx2. Alg2 silencing suppressed the expression of *Creb3l2* and chondrogenesis.
Conclusion: Alg2 may be a modulator of osteochondrogenesis.
Significance: This is the first report to describe the association of an Alg gene with osteochondrogenesis.

Human immunodeficiency virus type 1 enhancer-binding protein 3 (*Hivep3*) suppresses osteoblast differentiation by inducing proteasomal degradation of the osteogenesis master regulator Runx2. In this study, we tested the possibility of cooperation of Hivep1, Hivep2, and Hivep3 in osteoblast and/or chondrocyte differentiation. Microarray analyses with ST-2 bone stroma cells demonstrated that expression of any known osteochondrogenesis-related genes was not commonly affected by the three Hivep siRNAs. Only *Hivep3* siRNA promoted osteoblast differentiation in ST-2 cells, whereas all three siRNAs cooperatively suppressed differentiation in ATDC5 chondrocytes. We further used microarray analysis to identify genes commonly down-regulated in both MC3T3-E1 osteoblasts and ST-2 cells upon knockdown of *Hivep3* and identified asparagine-linked glycosylation 2 (*Alg2*), which encodes a mannosyltransferase residing on the endoplasmic reticulum. The *Hivep3* siRNA-mediated promotion of osteoblast differentiation was negated by forced Alg2 expression. Alg2 suppressed osteoblast differentiation and bone formation in cultured calvarial bone. Alg2 was immunoprecipitated with Runx2, whereas the combined transfection of Runx2 and Alg2 interfered with Runx2 nuclear localization, which resulted in suppression of Runx2 activity. Chondrocyte differentiation was promoted by Hivep3 overexpression, in concert with increased expression of *Creb3l2*, whose gene product is the endoplasmic reticulum stress transducer crucial for chondrogenesis. *Alg2* silencing suppressed *Creb3l2* expression and chondrogenesis of ATDC5 cells, whereas infection of Alg2-expressing virus promoted chondrocyte maturation in cultured cartilage rudiments. Thus, Alg2, as a downstream mediator of Hivep3, suppresses osteogenesis, whereas it promotes chondrogenesis. To our knowledge, this study is the first to link a mannosyltransferase gene to osteochondrogenesis.

In skeletal development and bone remodeling, osteoblasts play major roles not only in bone formation but also in inducing the differentiation of bone-resorbing osteoclasts (1, 2). Runx2 is a critical transcription factor in osteoblast differentiation, as evidenced by Runx2 knock-out mice, which exhibit a complete lack of both intramembranous and endochondral ossification due to the absence of osteoblasts (3). Cleidocranial dysplasia, a human autosomal dominant inherited disorder of bone development, is characterized by hypoplasia of clavicles and abnormalities in cranial and facial bones and is caused by mutations in the *Runx2* gene (4, 5). Some genes, *e.g.* LDL receptor-related protein 5 (*Lrp5*), sclerostin (*Sost*), and human immunodeficiency virus type 1 enhancer-binding protein 3 (*Hivep3*), have been found to control osteoblast function in the adult human and/or mouse during postnatal skeletal remodeling (6–10).

Hivep3, also known as Schnurri-3, Zas3, and Krc, is a member of three mammalian homologs of the Hivep/Schnurri family of large zinc finger proteins. Hivep proteins have been studied for their roles in the regulation of an assortment of genes, including those encoding collagen type IIA, αA-crystallin, β-interferon, and HIV genes (11). Hivep2 can indirectly interact with the peroxisome proliferator-activated receptor γ2 (*Pparg2*) promoter to promote adipogenesis, through binding to Smad1, an intracellular mediator of bone morphogenetic protein (BMP)[2] signaling. Hivep2 can also dock to CCAAT/enhancer-binding protein α (C/ebpα) to interact

* This work was supported by Japan Society for the Promotion of Science KAKENHI Grants 23592221 (to S. M.) and 23592222 (to Y. I.), a grant from the Cell Science Research Foundation (to S. M.), and a grant from the Hip Joint Foundation of Japan (to S. M.).
[S] This article contains supplemental Tables 1–5.
[1] To whom correspondence should be addressed: Dept. of Medical Joint Materials, Graduate School of Medical and Dental Sciences, Kagoshima University, 8-35-1 Sakuragaoka, Kagoshima 890-8544, Japan. Tel.: 81-99-275-5381; Fax: 81-99-265-4699; E-mail: maeda-s@umin.ac.jp or s-maeda@m3.kufm.kagoshima-u.ac.jp.

[2] The abbreviations used are: BMP, bone morphogenetic protein; ER, endoplasmic reticulum; ALP, alkaline phosphatase; ECM, extracellular matrix; CDG, congenital disorders of glycosylation; qRT, quantitative RT; ALG, asparagine-linked glycosylation.

with a CCAAT site on the distal part of the *Pparg* gene (12). Mice lacking Hivep3 demonstrate adult-onset osteosclerosis with increased bone volume due to enhanced osteoblast activity (10). Hivep3 promotes proteasomal degradation of the Runx2 protein through recruitment of the E3 ubiquitin ligase Wwp1 to Runx2 (10). A D-domain motif within Hivep3 mediates the interaction with and inhibition of ERK mitogen-activated protein kinase (MAPK), thereby inhibiting Wnt/Lrp5 signaling through regulation of the activity of a downstream mediator glycogen synthase kinase 3-β (Gsk3β). This interaction results in the suppression of subsequent osteoblast differentiation (13). In addition, Hivep3 indirectly promotes osteoclastogenesis by promoting osteoblastic expression of receptor activator of nuclear factor-κB ligand (Rankl), a crucial factor for osteoclast differentiation (14). Hivep3 also cell-autonomously promotes osteoclastogenesis by inducing the expression of *Nfatc1*, a master transcription factor in osteoclast differentiation, by interacting with Traf6 to enhance its activity while forming a complex with c-Jun to activate the *Nfatc1* promoter (15). Thus, Hivep3 controls both bone formation and resorption at multiple steps to maintain normal bone mass. However, whether Hivep3 controls gene expression in osteoblasts to regulate osteoblast activity is unclear.

In contrast to *Hivep3* knock-out mice, mice lacking *Hivep2* exhibited decreased cortical bone volume and increased cancellous bone mass (16), suggesting different roles for Hivep2 and Hivep3 in the skeleton. Combined ablation of *Hivep2* and *Hivep3* in mice resulted in synergistically increased trabecular bone volume, demonstrating a redundancy between the two proteins in the regulation of postnatal bone mass (17). Interestingly, in the double knock-out mice, the growth plate cartilage of the long bones was uncoupled with bone phenotype, with significantly delayed maturation of chondrocytes resulting in chondrodysplasia (17), suggesting a role for Hivep proteins in the promotion of chondrocyte differentiation. However, the mechanism by which Hivep proteins affect chondrogenesis remains unknown. In addition, to date, no information has been reported on the possible role of Hivep1 in osteogenesis and/or chondrogenesis.

In this study, *in vitro* analysis showed that, among the three Hivep proteins, only Hivep3 was inhibitory and that the others promoted osteoblast differentiation. In contrast, all three Hivep genes seemed to support chondrocyte differentiation in BMP-2-induced ATDC5 cells, suggesting their redundancy in chondrogenesis. We found that asparagine-linked glycosylation 2 (*Alg2*) is commonly down-regulated in BMP-2-induced osteoblast differentiation in both MC3T3-E1 and ST-2 cells. Alg2 inhibited Runx2 activity without altering its protein level, resulting in suppression of osteoblast differentiation. Interestingly, in chondrogenesis of ATDC5 cells, Hivep3 induced the expression of cAMP-responsive element binding-protein 3-like 2 (*Creb3l2*), an endoplasmic reticulum (ER) stress transducer crucial for chondrogenesis (18), suggesting a possible role for Hivep3 in physiological mild ER stress. Alg2 was also decreased by *Hivep3* knockdown in ATDC5 chondrocytes, whereas silencing of Alg2 suppressed the expression of *Creb3l2* and chondrogenesis. To our knowledge, this study is the first to show a linkage between an asparagine-linked glycosylation mannosyltransferase gene and osteochondrogenesis.

EXPERIMENTAL PROCEDURES

Cell Culture and Differentiation—The mouse calvarial bone-derived osteoblast cell line, MC3T3-E1 (clone 4), and the mouse chondrogenic fibroblast cell line, C3H10T1/2, were obtained from the ATCC. The mouse bone marrow stromal cell line ST-2 and the mouse chondrogenic cell line ATDC5 were obtained from the RIKEN BioResource Center. MC3T3-E1 cells were cultured in minimum essential medium α (Invitrogen) containing 10% fetal bovine serum (FBS). ST-2 cells were cultured in RPMI 1640 medium (Sigma) containing 10% FBS. ATDC5 cells were cultured in Dulbecco's modified Eagle's medium (DMEM)/Ham's F-12 (1:1) (Invitrogen) containing 5% FBS. C3H10T1/2 cells were cultured in basal medium Eagle's (Sigma) with 2 mM L-glutamine and 10% FBS. COS-7 cells were purchased from RIKEN BioResource Center and maintained in DMEM supplemented with 10% FBS. All cell culture medium contained 100 units/ml penicillin G and 100 μg/ml streptomycin. Cell differentiation was induced by the addition of recombinant human BMP-2 (PeproTech) at a concentration of 300 ng/ml. Micromass culture of ATDC5 cells was performed as described previously (19) to accelerate the maturation of chondrocyte differentiation.

Alkaline Phosphatase (ALP) and Alcian Blue Staining—The activity of ALP secreted into the extracellular matrix (ECM) of cultured cells was visualized with an ALP staining kit (85L-3R, Sigma). Cartilaginous glycosaminoglycans produced in the ECM by cultured cells were stained with Alcian blue 8GX (Sigma).

RNA Interference—Dharmacon siRNA ON-TARGETplus SMARTpool, a mixture of four independent siRNAs against mouse *Hivep1*, *Hivep2*, *Hivep3*, and *Alg2*, and the control reagent were purchased from Thermo Scientific. siRNAs were transfected into cells using Lipofectamine RNAiMax (Invitrogen).

Real Time Quantitative PCR—Cells were lysed with TRIzol reagent (Invitrogen) to purify RNA, and 1 μg of total RNA was subjected to reverse transcription with the Verso cDNA kit (Thermo Scientific). The relative amounts of the gene transcripts were determined by real time quantitative PCR using SYBR premix Ex TaqII (Takara) and the Thermal Cycler Dice TP850 system (Takara). PCRs were performed in duplicate per sample, and the measured expression level of each gene was normalized to that of *Hprt1*. The sequence information for the primers used is listed in supplemental Table 1. All primer sets are for mouse genes, except for the m/h*Hivep3* primer set, which can be used to amplify both the mouse and human *Hivep3* genes. For evaluation of the tissue distribution of the Hivep genes and Alg2 *in vivo*, tissues were harvested from 3-month-old mice, and mRNA was purified with TRIzol reagent before subjecting samples to qRT-PCR.

Microarray Analysis—Cells transfected with siRNA overnight were further incubated with BMP-2 for 2 days before being lysed with TRIzol reagent for mRNA purification. mRNA samples were cleaned up using the RNeasy MinElute Cleanup kit (Qiagen) and analyzed on a Mouse Gene 2.0 ST Array (Affymetrix) by BioMatrix Research.

Plasmids, Adenovirus, and Lentivirus—The mouse Hivep3 expression plasmid, pEF-Shn3, was a kind gift from Dr. Laurie Glimcher (Harvard Medical School). The human HIVEP3 expression plasmid pFN21A-HIVEP3 was obtained from Kazusa DNA Research Institute. The mouse type II Runx2 expression plasmid was a kind gift from Dr. Toshihisa Komori (Nagasaki University). The FLAG-Runx2-def expression plasmid has been described in our previous study (20). Mouse *Alg2* or *Runx2* cDNA was cloned from ST-2 cells by using a RT-PCR-based technique, subcloned into the entry vector, pENTR, and further transferred into the C-terminally V5-tagged expression vector, pEF-DEST51 (Invitrogen). For overexpression assays, cells were transfected with expression vectors using FuGENE 6 (Roche Applied Science) or Lipofectamine 2000 (Invitrogen). Cells transiently expressing the transgenes were selected and enriched by incubation with G418 disulfate (Nacalai Tesque) at a concentration of 250 μg/ml for 3–7 days. To generate adenovirus-carrying *Alg2* cDNA, the *Alg2* gene in the pENTR-Alg2 vector was transferred into the C-terminally V5-tagged adenovirus expression vector pAd/CMV/V5-DEST by LR recombination (Invitrogen) and was further transfected into the adenovirus-producing cell line 293A according to the manufacturer's protocol. The pAd/CMV/V5-GW/lacZ adenovirus expression vector was used to generate a control adenovirus. For generation of lentivirus carrying the *Alg2* gene, pENTR-Alg2 and pENTR-5′EF1αP were subjected to LR recombination with pLenti6.4/R4R2/V5-DEST (Invitrogen) to generate a lentiviral vector expressing C-terminally V5-tagged Alg2 from the EF1α promoter. The lentiviral expression vector or pLenti6/V5/GW-lacZ control vector was transfected into 293FT cells to generate the lentivirus. Virus infection into ST-2 cells was performed at a multiplicity of infection of 100. Cells infected with the lentivirus were selected by treatment with blasticidin S HCl (Invitrogen) at a concentration of 2.5 μg/ml. These experiments were approved by the Kagoshima University safety control committee for gene recombination techniques (number 22053).

Embryonic Bone Organ Culture—Calvarial bone and metatarsal bone (cartilage) rudiments were harvested from C57BL/6J mouse embryos at 17.5 days post-coitum (E17.5) and cultured in minimum essential medium α or DMEM/Ham's F-12 (1:1), respectively, supplemented with 10% FBS, 100 units/ml penicillin G, and 100 μg/ml streptomycin, as described (21). The bone rudiments were incubated in virus solution overnight for infection of adenovirus or lentivirus. Cultured bones and cartilages were fixed in 96% ethanol and stained with 0.015% Alcian blue 8GX in a mixture solution of 96% ethanol/acetic acid (4:1) for 1 day, followed by a dehydration step in 100% ethanol. Dehydrated bones were immersed briefly in 1% potassium hydroxide (KOH), followed by staining in 0.001% alizarin red S (Sigma) in 1% KOH for 1 day. Images were captured with stereomicroscope M165FC (Leica). The animal experiments were approved by the Institutional Animal Care and Use Committee of Kagoshima University (number MD12137).

Immunoprecipitation and Immunoblotting—For immunoprecipitation assays, COS-7 cells were transfected with Alg2-V5 and/or FLAG-Runx2 plasmids and were lysed in M-PER lysis buffer (Thermo Scientific) supplemented with aprotinin and phenylmethylsulfonyl fluoride (PMSF). The lysate was immunoprecipitated with anti-FLAG M2-agarose affinity gel (A2220, Sigma), and the M2 antibody-bound protein complex was eluted by incubation with 3×FLAG peptide (F4799, Sigma), according to the manufacturer's protocol. For immunoblotting assays, cells were lysed in either M-PER or NE-PER lysis buffer (Thermo Scientific) supplemented with aprotinin and PMSF or directly with 1× SDS sample buffer. SDS-PAGE, membrane transfer, and chemiluminescence were performed using a standard protocol. The blots were incubated with primary antibodies against Alg2 (1:1000; LS-C81338, Lifespan Biosciences), Runx2 (1:200; M-70, sc-10758, Santa Cruz Biotechnology), Runx2 (1:1000; 8G5, MBL), Sp7 (1:1000, ab22552, Abcam), Ibsp (1:1000, LS-C190916, Lifespan Biosciences), type II collagen (1:1000, LS-C175971, Lifespan Biosciences), Creb3l2 (1:1000, ab76856, Abcam), V5 (1:5000; R960-25, Invitrogen), FLAG (1:1000; M2, F1804, Sigma), and tubulin (1:1000; DM1A, T9026, Sigma) and with horseradish peroxidase (HRP)-conjugated anti-rabbit and anti-mouse secondary antibodies (1:10,000) (Cell Signaling). For examination of half-life of Runx2 protein, after overnight transfection with siRNA of *Hivep3*, ST-2 cells were treated with cycloheximide (Sigma) at 100 μg/ml, followed by immunoblotting using anti-Runx2 antibody. Signals were detected using the LAS 4000 mini image analyzer (Fujifilm).

Immunofluorescence—For immunofluorescence assays, cells transfected with Runx2 and/or Alg2-V5 expression plasmids were fixed with 4% paraformaldehyde in PBS for 30 min and treated with 0.2% Triton X-100. CAS block (Zymed Laboratories Inc.) was used for blocking. Cells were incubated with anti-Runx2 (1:100; 8G5, MBL), Alexa Fluor 568 rabbit anti-mouse IgG (1:1000; A11061, Invitrogen), and anti-V5-FITC (1:500; R619-25, Invitrogen) antibodies. Nuclei were stained with Hoechst dye (Invitrogen). Confocal fluorescent imaging was performed and analyzed using a laser scanning microscope system (LSM 700, Zeiss). For confirmation of the efficiency of virus infection in cultured bones, formalin-fixed mouse E17.5 embryo calvariae or metatarsal bones were embedded in paraffin blocks, which were sliced at a 4-μm thickness. The antigen was retrieved by Liberate Antibody Binding (L.A.B.) solution (Polysciences). A CAS block was used for blocking. Bone sections were incubated with anti-V5-FITC antibody. Images were captured with microscope AX80 and digital camera DP70 (Olympus).

Luciferase Assay—COS-7 cells or ST-2 cells were seeded in triplicate in 24-well plates and transiently transfected with the 6×OSE2 luciferase reporter plasmid (a kind gift from Dr. Toshihisa Komori), the mutant 6×OSE2 luciferase reporter plasmid (a kind gift from Dr. Gerard Karsenty, Columbia University Medical Center), the pGL4.75hRlucCMV *Renilla* vector (Promega), and expression vectors for Runx2, Alg2, or Hivep3. Dual-Luciferase assays were performed as described earlier (20) by using the GloMax 96 microplate luminometer (Promega).

Statistical Analysis—The data in this study have been expressed as mean ± S.D. values of three independent experiments. Statistical comparisons between the different treatments were performed using an unpaired Student's *t* test in